①

National   Defense
Defence   nationale
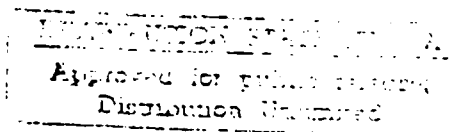
THE PERFORMANCE OF SPACE-BASED RADARS ORBITING ON ELLIPTICAL ORBITS

by

D. Faubert and M.P. Kerr

DTIC
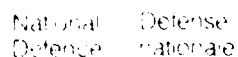ELECTE
MAR 2 8 1989
S D
D

DEFENCE RESEARCH ESTABLISHMENT OTTAWA
REPORT NO. 995

Canada

December 1988
Ottawa

89 3 28 009

THE PERFORMANCE OF SPACE-BASED RADARS ORBITING ON ELLIPTICAL ORBITS

by

D. Faubert and M.P. Kerr
Airborne Radar Section
Radar Division

Accesion For

NTIS

A-1

DEFENCE RESEARCH ESTABLISHMENT OTTAWA

REPORT NO. 995

ABSTRACT

The performance of Space–Based Radars (SBR) orbiting on elliptical orbits is discussed. Their ability to detect air–breathing targets is analyzed as a function of the antenna look angle, the orbital parameters of the satellite, the number of radio pulses transmitted and the peak power of the radar.

The results show that the minimum detectable velocities of the SBR tend to degrade as the satellite aikroaches the apogee of its orbit. Depending on the orbital parameters of the satellite, the advantage of more extended coverage when the satellite is at the apogee of its orbit could be hindered by the poorer performance of the radar.

RÉSUMÉ

On étudie la performance de radars orbitant sur des orbites elliptiques. On analyse leur capacité à détecter des cibles aériennes en fonction de l'angle de visée de l'antenne, des paramètres orbitaux, du nombre d'impulsions radar transmises et de la puissance crête du radar.

Les résultats obtenus démontrent que la performance du radar se détériore à mesure que le satellite se rapproche de l'apogée de son orbite. L'avantage d'une meilleure couverture du système de surveillance vers l'apogée est souvent compromise par la performance réduite du système.

TABLE OF CONTENTS

1.0 INTRODUCTION

The use of Space–Based Radars (SBR) has been suggested to satisfy the exacting requirements of strategic surveillance. SBRs can provide day, night and all–weather operation, very fast response time and enormous coverage.

The Radar Division of the Defence Research Establishment Ottawa has an ongoing SBR program. The work performed to date consisted in evaluating the performance of SBRs orbiting on circular orbits (Refs. 1–8). It is well known that elliptical orbits can be used to optimize coverage over certain portions of the Earth's surface. By positioning the apogee of the orbit above the Canadian Artic for instance, it should be possible to provide more extensive coverage of this strategically critical region.

However, questions arise about the performance of an SBR orbiting on an elliptical orbit. Since the altitude of the satellite above the Earth's surface is a function of the position of the satellite along its orbit, the clutter power and the strength of the signal reflected by the targets vary as a function of the orbital position of the satellite. The studies cited earlier have indicated a strong link between the performance of the radar and the relative level of the target and the clutter power. It is thus reasonable to expect that the ability of an SBR to detect targets could vary significantly along the orbit of the satellite. The objective of this report is to investigate these effects and to discuss the performance of SBRs orbiting on elliptical orbits.

Section 2 provides an overview of the SBR model and describes the baseline SBR parameters. Section 3 contains an analysis of the performance of the baseline SBR system. Section 4 reports on a parametric investigation into the effect of various system parameters on the performance of the SBR. Section 5 summarizes the findings of this work.

2.0 SBR MODEL AND BASELINE SYSTEM

The results presented in this report were obtained using the model developed in Refs. 1–3. Since this model has been documented at length in the references, only a brief overview is given here.

2.1 Orbital Dynamics

The satellite is assumed to revolve around the earth along an elliptical orbit, as shown in Fig. 1. The position of the satellite (r, θ) as a function of time t can be derived

from Kepler's equations and is given by (Ref. 1):

$$(1) \qquad r = \frac{h^2/\mu}{1+e\ \cos\ f} = \frac{a\ (1-e^2)}{1+e\ \cos\ f}$$

$$(2) \qquad \theta = f$$

$$(3) \qquad \dot{r} = \frac{h\ e\ \sin\ f}{a\ (1-e^2)}$$

$$(4) \qquad \dot{\theta} = \dot{f} = h/r^2$$

where h is the angular momentum constant of the satellite, μ is the gravitational constant of the Earth (3.986×10^{14} m^2/s), e is the eccentricity of the orbit and where the rest of the parameters are defined in Fig. 1.
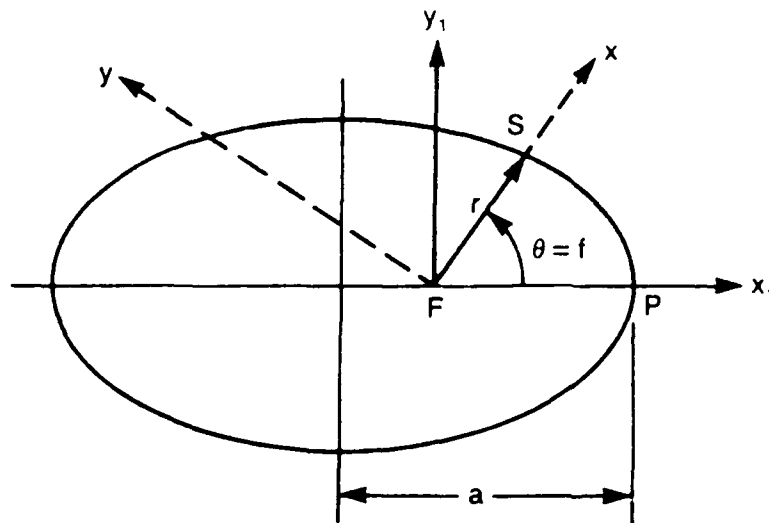

Fig. 1 Definition of the elliptical orbit parameters

The orientation of the orbit of the satellite with respect to a geocentric coordinate system is shown in Fig. 2. After Ref. 3, we restrict ourselves to polar orbits ($I=90°$) because, for circular orbits, the performance of SBRs depends only slightly on the inclination angle of the orbit. It is reasonable to assume that the same result applies for the case of elliptical orbits. We also assume that the longitude of the ascending node and the argument of the pericenter (Ω and ω in Fig. 2) are both equal to zero. Since the

earth is considered to be a featureless sphere, this can be done without loss of generality. Hence, the perigee of the orbit will always be located above the Greenwhich meridian, and over the equator.

Fig. 2 Definition of the orbital parameters

The position of the satellite with respect to a point on the earth's surface can be specified in a number of different ways. But since the Earth has been assumed to be a featureless sphere, it is sufficient to use the true anomaly (f in Figs. 1,2) to specify the position of the satellite along its orbit.

2.2 Radar model

The model developed in Refs. 1–3 uses the standard radar range equation to compute the strength of the signal from the target,

$$(5) \qquad S = \frac{n^2\ P_k\ \tau\ G^2\ \lambda^2\ \sigma_t}{(4\pi)^3\ R_t^4\ L_s}$$

4

where G is the gain of the antenna, τ is the compressed pulse width, n is the number of transmitted pulses integrated coherently, R_t is the range from the radar to the target and where the remaining symbols are defined in Table I.

TABLE I

BASELINE RADAR SYSTEM PARAMETERS

Apogee	5000 km
Perigee	500 km
Maximum radar peak power (P_k)	17 kW
Antenna diameter (D)	37.69 m
Wavelength (λ)	0.2 m
Pulse repetition frequency (PRF)	10,000 KHz
Pulse length uncompressed (τ)	50 μs
Compression factor (C)	82.021
System temperature (T_s)	490 K
System losses (L_s)	9 dB
Probability of detection (P_d)	90%
Probability of false alarm (P_f)	10^{-6}
Target model	Swerling II
Target cross section (σ_t)	20 m²
Altitude of target	0.0 km
Radar maximum range (R_{max})	9,422.3 km

The clutter power is evaluated by summing up the power contributed by all the clutter patches located on the ambiguous range lines within the footprint of the antenna. The clutter power is sorted out in the various frequency bins of a DFT processor by keeping track of the radial velocity of the clutter patches, v, with respect to the satellite. The expression giving the clutter power as a function of v is (Refs. 1–3)

$$(6) \qquad C(v) = \frac{P_k \, \tau \, G^2 \, \lambda^2}{(4\pi)^3 \, L_s} \sum_i \sum_j \frac{w_i^2}{R_i^4} \left(\frac{c \, \tau \, C_0 \, R_i \, \cos\theta_i \, \Delta\phi}{2 \, \cos \, \gamma_i} \right) \times$$

$$\sigma^0 (\gamma_i) \, G^2(\phi_i, \phi_{ij})$$

The symbol c is the speed of light, C_0 is the compression ratio, w_i is a weighting function, R_i is the range from the radar to the ith ambiguous range line, θ_i and ϕ_{ij} are the angles describing the location of the the jth clutter patch on the ith range line, γ_i is the grazing angle corresponding to the ith range line σ_0 is the surface backscattering coefficient and $\Delta\phi$ is the angular extent of a clutter patch.

The radial velocity of the i,jth clutter patch with respect to the radar is given by (Ref. 3)

$$(7) \qquad v_{ij} = (a^2+b^2)\cos(\phi_{ij}+A) + \dot{r}\left[1 - \frac{R_e^2}{R_i^2}\cos^2\gamma_i\right]$$

where R_e is the radius of the Earth and a,b and A are constants depending on the orbital parameters of the satellite (see Refs. 2,3). The noise equivalent power of the radar receiver, N_0, is given by

$$(8) \qquad N_0 = n\,k\,T_s$$

where k is the Boltzman constant and T_s is the system temperature.

The parameter used to evaluate the performance of the radar is the Signal–to–Interference Ratio (SIR). It is defined as

$$(9) \qquad SIR(v) = \frac{S}{C(v)+N_0}$$

where N_0 is the Noise Equivalent Power of the receiver. As defined in this report, the SIR is a function of the radial velocity of the target since $C(v)$ is a function of v. This is contrary to the standard definition of the SIR (Ref. 9) which defines the SIR as the average of the SIR over all possible radial velocities of the target. The definition adopted here enables us to determine the performance of the pulse Doppler radar as a function of the radial velocity of the target.

The orientation of the radar antenna is specified with respect to the North–East–Down (NED) frame of reference, centered on the satellite (see Refs. 2,3).

The antenna is taken to be oriented at an angle ϕ_1 with respect to the North axis of the NED system and at angle θ_1 with respect to the NE plane, as shown in Fig. 3. The angle ϕ_1 is called the azimuth–look angle and θ_1 is the look–down angle. The angle ϕ_1 is related to the grazing angle of the antenna, γ_1 as shown in Fig. 4. In the rest of this report, the look direction of the radar will be defined by using ϕ_1 and γ.
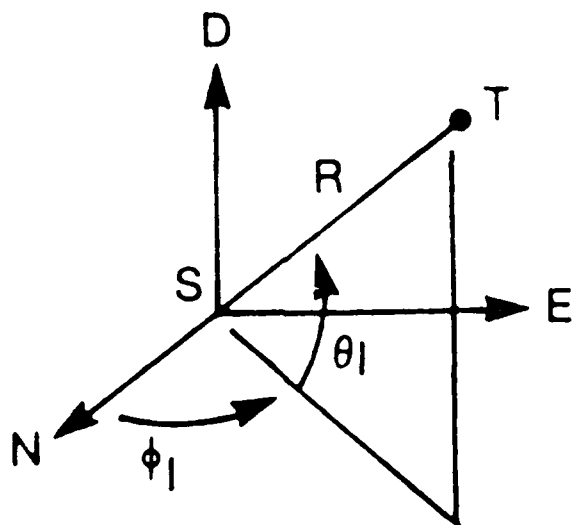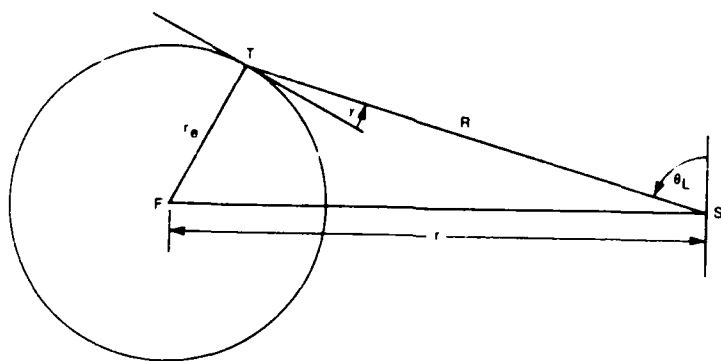
Fig. 3 Orientation of the antenna in the NED frame.

Fig.4 Relationship between the look–down and the grazing angles.

2.3 Baseline System Parameters

The radar system is designed in the manner described in Ref.3. To allow a direct comparison with the results obtained for circular orbits, the baseline radar parameters were chosen to equal those of Ref. 3 whenever possible.

The baseline system design procedure adopted in Ref. 3 can be summarized as follows. The peak power, the wavelength , the pikse repetition frequency, the pulse length, the compression factor, the system temperature, the probabilities of detection and of false alarm, and the design Signal—to—Noise Ratio (SNR) are selected from various system considerations (see Ref. 3). Then, the number of pulses in the burst, N_p, is chosen not to exceed N_{pmax}, which is related to the two way travel time to the surface of the earth by

$$(10) \qquad N_{pmax} = \frac{2\ R_t}{c} \times PRF$$

where R_t is the range to the target, which also equals the range from the radar to the surface of the earth along the axis of symmetry of the antenna. Finally, the diameter of the antenna is adjusted to achieve the design SNR at the maximum range of the radar (a point on the Earth's horizon).

For elliptical orbits, however, the two way travel time to the surface of the earth changes continuously as the satellite revolves around the earth. Consequently, R_t and N_{pmax}, which are linked by Eq. 10, vary along the orbit. There are a number of options to deal with this situation and all will be examined in this report. The first option consists of calculating N_p when the satellite is at the perigee and keeping it constant along the orbit. The size of the antenna is then adjusted to achieve the required SNR at the apogee. Under these conditions, it is readily seen from Eqs. 5 and 8 that the SNR of the radar at different positions along its orbit varies according to the following relationship:

$$(11) \qquad SNR \propto 1/R_t^4$$

The second option consists of allowing N_p to vary along the orbit. A longer burst can thus be transmitted when the satellite is at the apogee. Although the second option requires a more elaborate waveform generation system, it results in a smaller antenna to achieve the design SNR. Since N_p is proportional to R_t, the SNR of the system at different points along the orbit when option two is selected is proportional to

$$(12) \qquad SNR \propto 1/R_t^3$$

Since the SNR is designed to be met at the apogee, the last equation shows that it exceeds the design value when the satellite is away from the apogee. Thus, a third option is to decrease the peak power of the compressed radar pulses, in addition to allowing a variable burst length, in order to maintain a constant SNR along the orbit. The peak power of the compressed radar pulses would then be related to R_t according to

$$(13) \qquad P = P_k \left[\frac{R_t}{R_{max}} \right]^3$$

where R_{max} is the maximum range to the target when the satellite is located at the apogee of its orbit and P_k is the maximum allowable peak power for a duty cycle of 0.5. The advantage of the third option is to reduce the demand on the overall satellite system. This could help to increase the orbital duty cycle (the fraction of the orbit over which the SBR can be operated) by decreasing the power required from the batteries of the satellite. The second option is chosen to be the default option in this report. The two other options will be investigated in Section 5.

The orbit selected for the baseline system has an apogee of 5000 km and a perigee of 500 km (e=.2465). These parameters should not be regarded as optimal. They are only chosen for illustrative purposes. The choice of optimal orbital parameters requires a careful trade–off analysis which is beyond the scope of this paper.

A summary of the baseline SBR system appears in Table I. For more details about the design procedure of the SBR, Ref. 3 should be consulted.

3.0 PERFORMANCE OF THE BASELINE SBR SYSTEM

In this section, a detailed analysis is made of the performance of the SBR baseline system.

Fig. 5 shows the SIR of the radar as a function of the relative radial velocity, V_r, of the target. Positive and negative velocities are for approaching and receding targets respectively. The relative radial velocity $V_r=0$ corresponds to the radial velocity between the satellite and a clutter patch on the boresight of the radar antenna. The SIR curves are plotted versus the relative radial velocity, instead of the radial velocity, to facilitate the comparison between cases relating to different orbital parameters, and

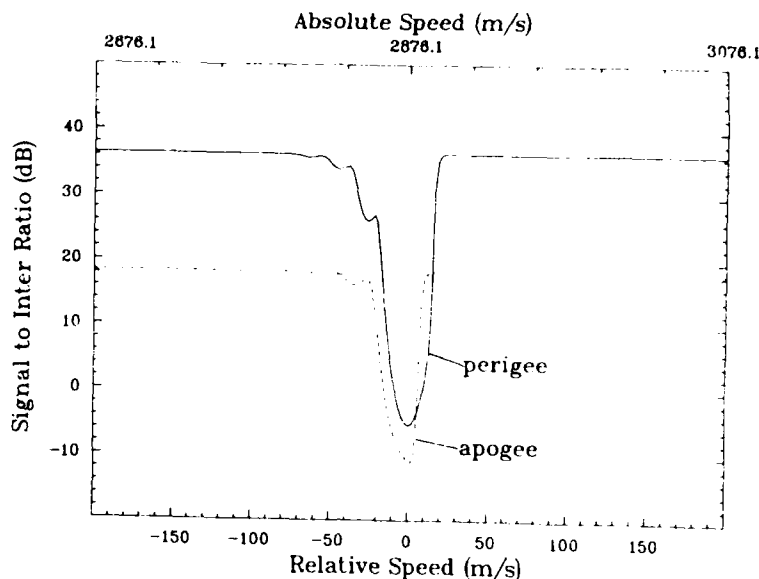different orientations of the radar antenna.

Fig. 5 SIR curves for the baseline system at a grazing angle of 3°.

The horizontal dotted line appearing in Fig. 5 represents the detection threshold of the system. If the SIR of the radar exceeds this threshold, the target will be declared present. The smallest absolute values of positive V_r, P_{mdv}, and of negative V_r N_{mdv}, beyond which the system exceeds the detection threshold are called the Minimum Detectable Velocities of the system. Targets travelling at velocities within the interval $[N_{mdv},P_{mdv}]$ cannot be detected while targets travelling at velocities outside this interval can be detected by the SBR. The $[N_{mdv},P_{mdv}]$ interval is used as a measure of performance of the SBR since a smaller $[N_{mdv},P_{mdv}]$ interval implies a narrower range of target velocities over which the SBR is ineffective, and consequently a better system performance.

The SIR curves of Fig. 5 can be more easily interpreted by considering two limiting cases. For $|V_r|$ very large, the clutter interference is small and the SIR reduces to the SNR of the system. Fig. 5 shows that for large $|V_r|$ the SNR is approximately 18 dB larger when the satellite is at the perigee than when it is at the apogee. This is consistent with Eq. 12 since at the perigee, R_t=2262.41 km while R_t=9094.26 km at the apogee.

For $|V_r|$ very small, the clutter interference is much larger than the noise equivalent power and the SIR reduces to the Signal to Clutter Ratio (SCR) of the system. Fig. 5 shows that the SCR is approximately 6 dB larger when the satellite is at the perigee than when it is at the apogee. This result may appear surprising at first if one considers only the clutter interference, $C(v)$, arising from the clutter patch which is boresighted with the radar antenna. Since the target is also assumed to be boresighted with the antenna, the ratio of the target power to the power returned by the boresighted clutter patch should not change along the orbit. However, the total clutter interference is made up from the contribution of all the clutter elements within the footprint of the antenna, as given by Eq. 6, and $C(v)$ does vary along the orbit. This is explained as follows. As the satellite is moving toward the apogee, R_t increases, and the footprint of the antenna increases according to R_t^2. Also, for a larger R_t and for a given look direction of the antenna, the ambiguous range lines are closer together on the surface of the earth. Finally, as R_t increases N_p increases and more range lines can contribute to the clutter return. These three effects tekd to increase the magnitude of the clutter return as R_t increases. There is also a balancing effect, since as R_t and consequently N_p increase, the width of the DFT filters used in the receiver decreases as R_t^{-1}. This reduces the clutter interference at a given relative velocity. Unfortunately, the rather complicated form of Eq. 6 prevents us from establishing a proportionality relationship between SCR and R_t. But the arguments invoked above explain qualitatively the higher SCR for small $|V_r|$ when the satellite is at the perigee.

The SIR curve of Fig. 5 exhibits a sharp cut-off on the positive side of the abcissa of the SIR curve. This effect has been explained in previous publications (Refs. 1-3). It occurs when the antenna is pointed at a small grazing angle, in the look ahead mode (small θ_1). In these cases, a significant portion of the footprint of the antenna is over the Earth's horizon. This causes an abrupt cut-off of the clutter power contributed at relative velocities larger than the velocity of a clutter patch located on the Earth's horizon. This effect disappears rapidly as γ_1 and ϕ_1 increase.

The MDVs for the baseline case can be evaluated from Fig. 5. They equal [-16,12] and [-43,9] for the perigee and the apogee cases respectively. Because of the sharp cut-off of the clutter power for the positive relative velocities, the P_{mdv}'s are approximately equal when the satellite is at the perigee or at the apogee. But the N_{mdv} is approximately 2.6 times larger at the apogee than at the perigee.

Fig. 6 shows the SIR curves of the SBR at four different positions along its orbit. The trends described above can still be observed in the figure. The further away the satellite is from the Earth's surface, the lower are the SNR and the SCR of the system.
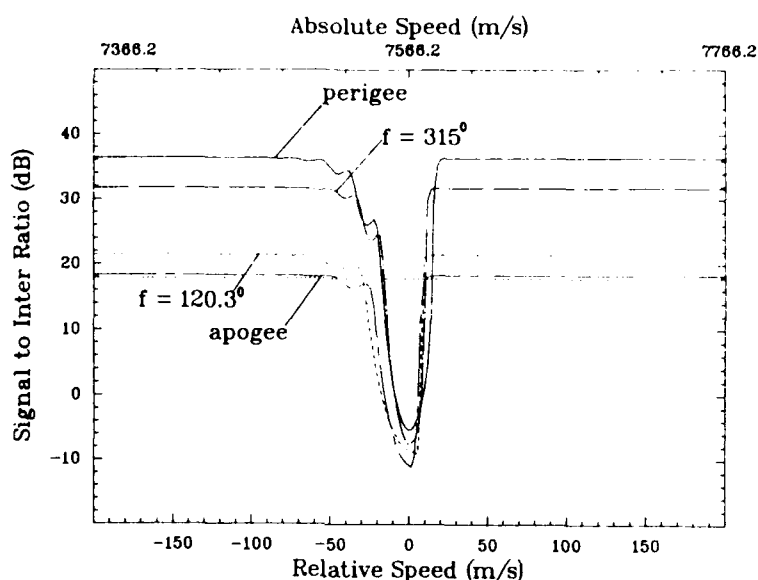

Fig. 6 SIR curves for the baseline system at various locations along its orbit.

Fig. 7 shows the SIR curves of the SBR when it is located above the north and the south poles (f=90° and 270° respectively). Although the satellite is at the same distance from the Earth surface in these cases, the SIR curves are significantly different. This can be explained with the help of Eqs. 3, 4 and 7. Eq. 4 shows that the tangential velocity of the satellite,$d\theta/dt$ is the same at both points of the orbit. But Eq. 3 shows that the velocity of the satellite with respect to the center of the earth, dr/dt, is positive when the satellite is above the North pole (f=90°), but negative when the satellite is above the south pole (f=270°). This results in different v_{ij} as given by Eq. 7 and consequently different clutter spectra. It should be noted, however, that if the antenna was pointed in the direction opposite to the motion of the spacecraft (ϕ_1=180°) say at the North pole, its SIR curve would be the mirror image of the one obtained in the look ahead mode (ϕ_1=0°) above the South pole.
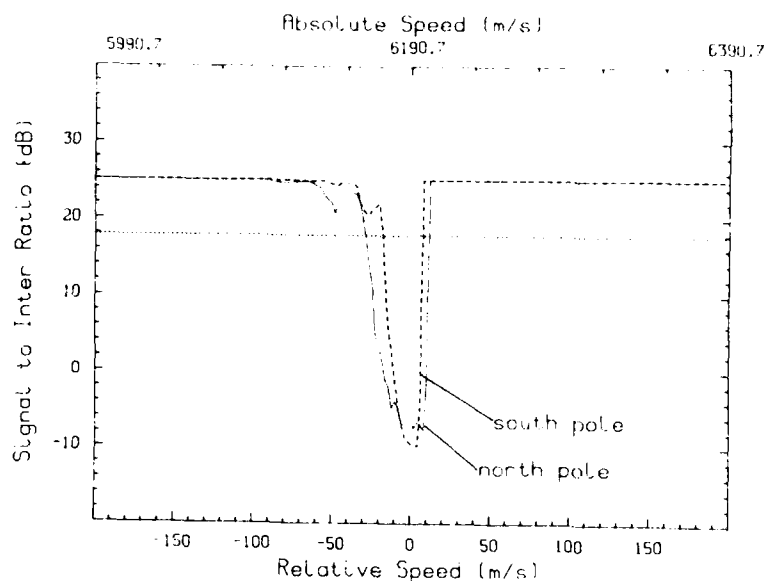
Fig. 7 SIR curves for the baseline system at the apogee and the perigee

Fig. 8 shows the MDVs of the baseline SBR system as a function of the orbital position of the satellite. Due to the sharp cut—off of the clutter power on the positive side of the velocity axis of the SIR curves, P_{mdv} is relatively constant as a function of the position of the satellite. However, N_{mdv} changes significantly along the orbit. Thus, at least for the orbital parameters investigated here, the performance of the radar, in terms of the MDVs, will degrade significantly as the satellite moves toward the apogee. This might seriously hinder any advantage gained from improved coverage of a given geographic area as the satellite reaches the apogee.
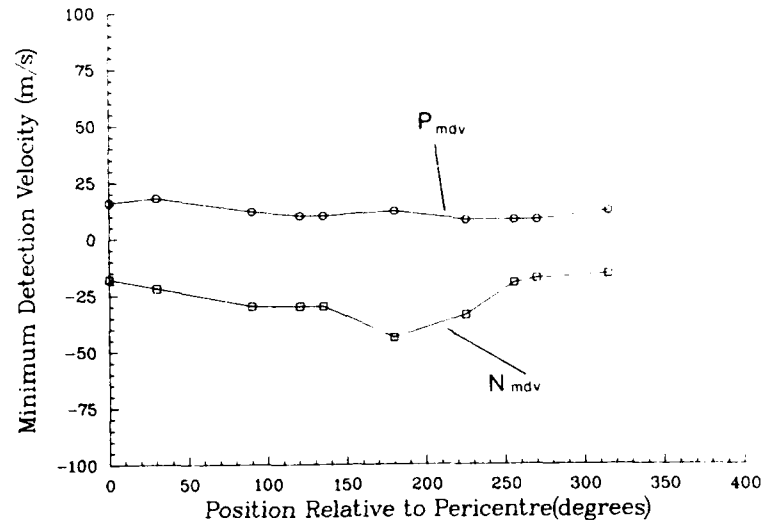
Fig. 8 MDVs of the baseline system.

4.0 PARAMETRIC INVESTIGATION

In this section, we present results indicating how the performance of an SBR orbiting on an elliptical orbit changes when some system parameters are changed.

4.1 Effect of the look direction of the antenna

As discussed in Ref. 3, significant changes in the shape of the clutter spectra occur when the look direction of the antenna is changed. For a fixed grazing angle, Ref. 3 has shown that the clutter spectrum broadens as the azimuth look angle, ϕ_1, increases from 0° to 90°, resulting in poorer MDVs. The effect of ϕ_1 is the same for an SBR on an elliptical orbit. The reader is referred to Ref. 3 for a detailed discussion on the subject.

For a fixed ϕ_1, the clutter spectrum also varies considerably as a function of γ_1. Fig. 9 shows the SIR curve for the baseline SBR system for $\gamma_1=60^\circ$. Comparing Fig. 9 to Fig. 5 for which $\gamma_1=3^\circ$, it is observed that the shape of the SIR curves and the MDVs of the system change as a function of γ_1. Moreover, Fig. 9 shows that for a steep

14

grazing angle, the shape of the SIR curve changes as a function of the orbital position of
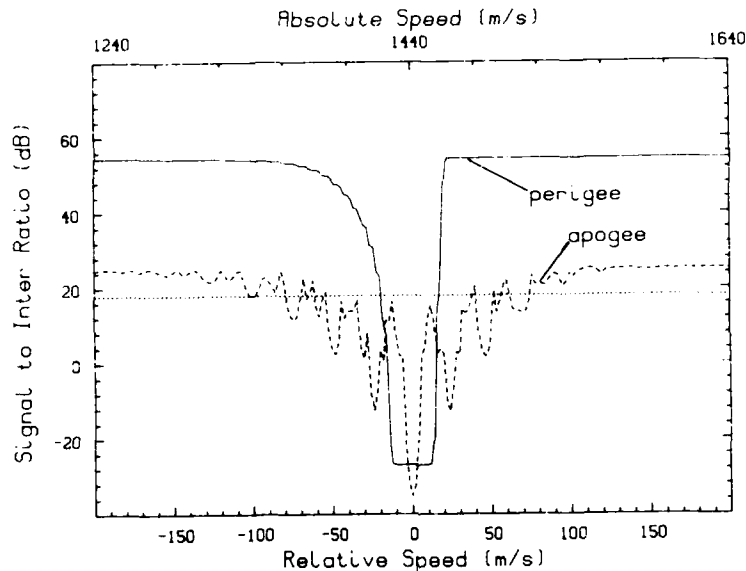the satellite. This was not the case for a lower value of the grazing angle, as seen in Fig.
5.

Fig. 9 SIR curves for the baseline system for a grazing angle of 60°

The effect of the grazing angle on the clutter spectra of an SBR orbiting on a
circular orbit has been discussed in Ref. 3. The same considerations apply here and will
be reviewed briefly. As γ_1 increases, the range to the surface of the earth, R_t, decreases.
This results in an increase of the strength of the clutter return and of the signal from the
target. Also, the size of the footprint of the antenna which is proportional to R_t^2
decreases as γ_1 increases. Finally, the spacing between the ambiguous range lines
increases with γ_1. These effects tend to reduce the width of the clutter spectrum and
consequently lower the MDVs. More specifically for the case of Fig. 9 at the perigee,
the footprint of the antenna is relatively small and the ambiguous range lines are far
enough apart that only one range line contributes significantly to the clutter return.
This results in a relatively narrow clutter spectrum and SIR curve. But when the
satellite is at the apogee, the area of the footprint of the antenna is approximately 16
times larger than at the perigee. More range lines contribute to the clutter spectrum,

resulting in a broader SIR curve.

The MDVs are [−20,16] and [−102,74] when the satellite is at the perigee and the apogee respectively. Hence, for $\gamma_1=60^\circ$, the MDVs change by a factor of almost five as the satellite moves along its orbit. Clearly, the advantage of better coverage at the apogee of the radar might be seriously hindered by a poorer radar performance if the antenna were pointed at a steep grazing angle.

4.2 Effect of the Eccentricity of the Orbit

This section discusses the effect of the orbital parameters of the satellite on the performance of the radar. It might be expected that the effects discussed in the preceding sections become more pronounced as the eccentricity of the orbit increases. This is not necessarily the case since the performance of the radar results from a very complex set of interactions between the orbital parameters, the radar parameters and the geometry of the problem. Since some radar parameters change when the orbital parameters are altered in order to maintain a constant design SNR, it is difficult to predict the performance of the radar for different orbital parameters.

The problem of varying the orbital parameters of the satellite to investigate their effects on the performance of the radar is in itself not trivial. But fortunately, there are some considerations applicable to SBR which help restrict the range of orbital parameters which can be chosen. The perigee of the orbit must not be much lower than a few hundred kilometers to avoid excessive atmospheric drag. Also, the antenna size required to achieve the design SNR increases very rapidly as the apogee increases. In this report, we thus impose a maximum apogee of 10,000 km resulting in an antenna size of approximately 50 m to detect a bomber size target located at the Earth's horizon. We also fixed the perigee of the orbit at 500 km in all cases.

Fig. 10 shows the SIR curves when the satellite is at the apogee of three different elliptical orbits and the circular orbit investigated in Ref. 3. The four curves have similar shapes but become narrower as the apogee increases. This results from a number of factors and Table II is provided to illustrate their relative importance. F_{8i} higher apogees, the velocity of the satellite is lower. Also, the antenna is larger which causes a narrower beamwidth. These effects result in a narrower clutter spectrum, as is shown next.

TABLE II

SBR SYSTEM PARAMETERS FOR VARIOUS ORBITS

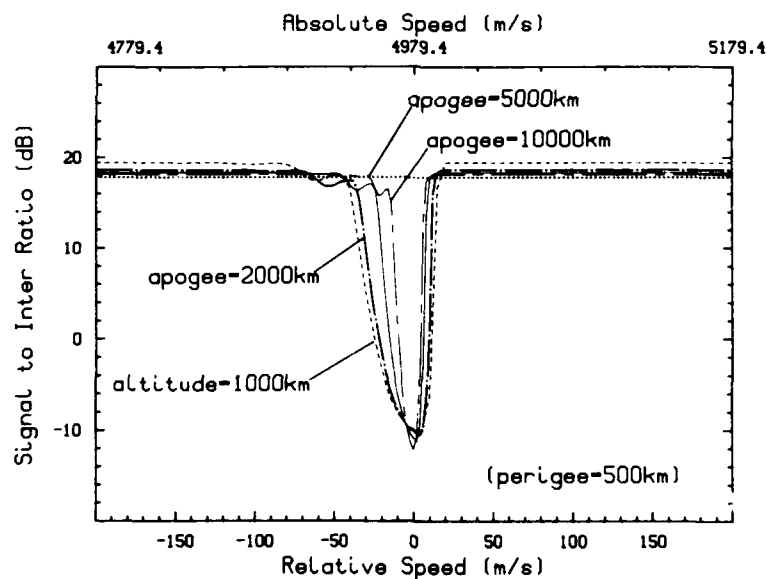| Apogee (km)	Perigee (km)	e	Apogee Rt (km)	Vtg (*)	Perigee Rt (km)	Vtg (*)	D (m)
10 000	500	0.4085	16378	3.79	6878	9.03	52.34
5000	500	0.2465	9128	5.14	6878	8.49	37.69
2000	500	0.0983	7628	6.55	6878	7.98	14.40

(*) Relative Units

Fig. 10 SIR curves for various orbital parameters.

Let V_{tg} be the velocity component of the satellite which is tangential to the surface of the earth and β be the beamwidth of the antenna measured between the 3dB points of its radiation pattern. The width of the clutter spectrum, $\Delta\nu$, is approximately given by the difference between the Doppler shifted frequencies of the leading and the trailing edges of the beam. If the antenna is oriented at an angle θ with respect to the velocity vector of the satellite, $\Delta\nu$ is approximately given by

$$(14) \qquad \Delta\nu = \frac{2\,V_{tg}}{\lambda}\left[\cos\left(\theta - \beta/2\right) - \cos\left(\theta + \beta/2\right)\right]$$

For β small, Eq. 14 can be simplified to

$$(15) \qquad \Delta\nu = \frac{2\,V_{tg}}{\lambda}\,\beta\sin\theta$$

The last equation shows that the reduction in the velocity of the satellite at higher apogees and the narrower beamwidth of the antenna reduce the width of the clutter spectrum proportionally. Moreover, as R_t increases the transmitted burst length increases, which results in a bank of narrower DFT filters in the radar receiver. These effects are somewhat offset by the higher density of the range lines at longer ranges to the Earth surface. Although it is not possible to establish a simple proportionality between the width of the clutter spectrum and the apogee of the orbit, the arguments given above and in Table II explain the narrower SIR curve of Fig. 10.

Fig. 11 shows the MDVs of the SBR at different points along the four orbits used in Fig. 10. The PMDVs are fairly constant along the orbit because of the sharp cutoff of the clutter spectrum on the positive side of the velocity axis of the SIR curves for low grazing angles. On the other hand, Fig. 11 shows that as the apogee of the orbit increases, the NMDVs improve, for any position of the satellite along its orbit. As explained above, this is because the clutter spectrum is narrower as the apogee of the orbit increases. Fig. 11 also shows that the ratio between the maximum and the minimum MDVs which occur, as before, at the apogee and the perigee of the orbit respectively, decreases as the apogee becomes higher. This can be explained using Table II. At the perigee, Table II shows that the velocity of the satellite is fairly constant for the various elliptical orbits. Also, since the perigee is the same for each elliptical orbit,

18

R_t is the same in all cases and the number of pulses transmitted in the burst and the density of the range lines is the same. But a significant reduction of the width of the clutter spectrum is achieved as the antenna size becomes larger to accommodate higher apogees. Hence, although the difference between the velocity of the satellite at the apogee and the perigee increases as the apogee gets higher, the larger antenna size required to achieve the design SNR smooths the MDV versus f curve.
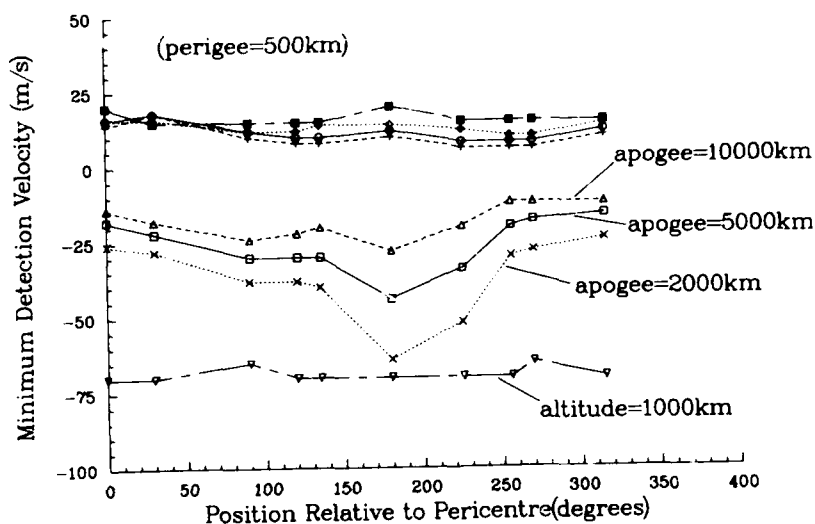

Fig. 11 P_{mdv} (upper curve) and N_{mdv} (lower curve) for various orbital parameters.

In summary, there is always variation in the MDVs of the SBR as a function of the orbital position of the satellite, even for a circular orbit, as shown in Fig. 11. These differences are more pronounced at larger grazing angles. They tend to even out as the apogee of the orbit increases, but at the expense of much larger antenna sizes.

4.3 Variable Burst Length

Section 2 of this report pointed out that two SBR parameters, namely N_p and P_k, could be selected according to three different criteria. In the preceding sections, we have investigated the performance of the SBR when option two was selected. For this case, the peak power of the compressed radar pulses is kept constant along the orbit but the duration of the burst of pulses is adjusted along the trajectory of the satellite to maximize the value of N_p. Fig. 12 shows MDVs of the baseline system if option one is selected. In this case, P_k is fixed along the trajectory of the satellite and N_p, computed at the perigee of the satellite, is kept constant along the orbit. Fig. 12 shows that the performance of the radar does not differ significantly in the two cases. The SBR with constant N_p performs somewhat better toward the perigee because of the larger antenna size it requires to achieve the design SNR. On the other hand, the SBR with variable N_p performs a little better toward the apogee because of its higher frequency resolution resulting from a longer burst of pulses.
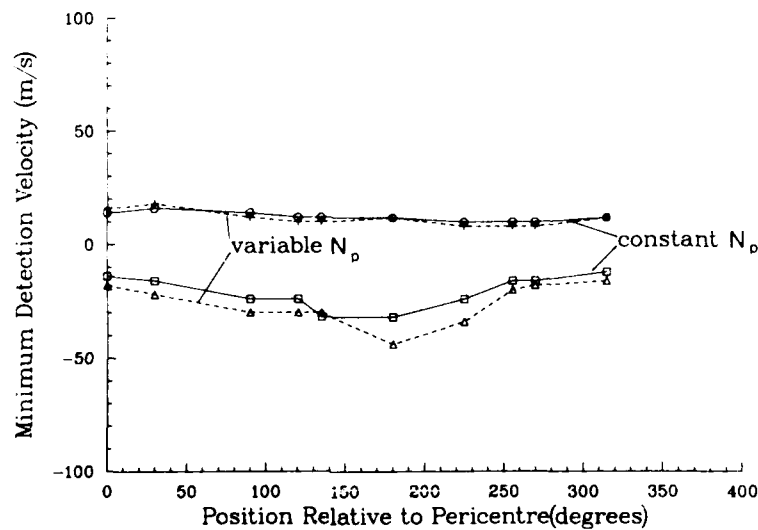

Fig. 12 P_{mdv} (upper curve) and N_{mdv} (lower curve) for the fixed and the variable burst lengths.

The real advantage of a variable burst length, however, lies in its requirement for a smaller antenna. Fig. 13 compares the required antenna sizes as a function of the apogee of the satellite when the SBR is designed according to options one and two. Clearly, the significantly smaller apertures of the variable N_p option makes it preferable to the fixed burst length option.
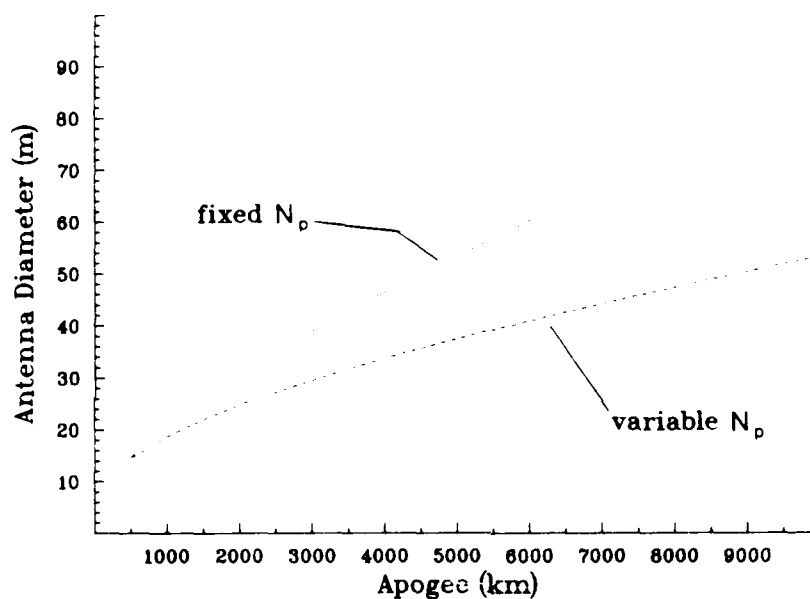

Fig. 13 Antenna diameter for the fixed and the variable burst lengths.

The third option proposed at the beginning of this report allowed for an adjustement of P_k in addition to varying N_p along the orbit of the SBR. Fig. 14 shows the MDV of the baseline system as a function of the position of the satellite for a variable P_k and N_p. As expected, the performance is equal at the apogee but degrades significantly towards the

perigee as the power is reduced to maintain a constant SNR along the orbit. However, at the perigee, the power was reduced by a factor of 18.13 dB (64 times). Thus if the degradation of the performance of the SBR is acceptable, considerable power savings could be achieved. Since the orbital duty cycle is a strong limiting factor for SBR systems, a variable P_k should be considered in a detailed trade—off study of a practical SBR configuration.
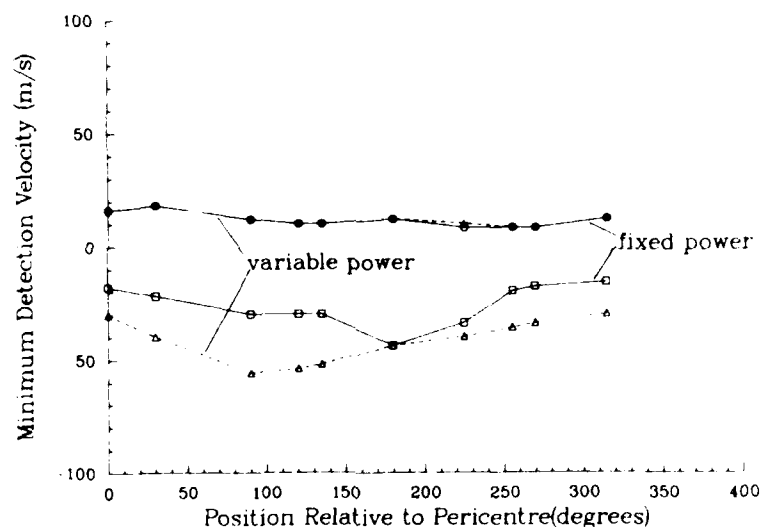

Fig. 14 P_{mdv} (upper curves) and N_{mdv} (lower curves)for the fixed and the variable power cases.

5.0 CONCLUSION

The performance of an SBR orbiting on an elliptical orbit varies as a function of the orbital position of the satellite. The MDVs of the radar become poorer as the satellite moves toward the apogee of the orbit. This effect is much more pronounced when the antenna of the radar is pointed at steep grazing angles. As the apogee of the orbit increases, the performance of the radar is more uniform as a function of orbital position. However, this is achieved at the expense of a much larger antenna size.

Varying the number of pulses in the transmitted burst as a function of the orbital position of the satellite allows for a much smaller antenna without a significant degradation in the performance of the SBR. The variation in the peak power of the radar as a function of the orbital position of the satellite should also be considered to increase the orbital duty cycle.

Regardless of other advantages and disadvantages of elliptical orbits, their use to improve the coverage of a strategic surveillance system may result in a significant degradation in the performance of the radar toward the apogee of the orbit, depending on the orbital parameters of the satellite. Since this degradation occurs precisely where it is desired to improve coverage, the use of elliptical orbits for SBR systems will involve a careful trade—off analysis between coverage and target detection capability.

6.0 REFERENCES

1. Bird, J. S., and A. W. Bridgewater, "Performance of Space—Based Radars in the Presence of Earth Clutter", IEE Proc. Vol 131, Pt. F. No. 5, August 1984, pp. 491–500.

2. Rook, B. J., J. Bird and A. W. Bridgewater, "Detection of Near Earth Targets by Space—Based Radars: Development and Use of Computer Simulations", CRC Report No. 1389, 1985.

3. Faubert, D., B. J. Rook and W. Tam, "Analysis of Space—Based Radar Clutter Spectra Over Different Types of Terrain and Their Effects on Detection Performance, CRC Report 1408, November 1986.

4. Tam, W. and D. Faubert, "A Theory of Displaced Phase Center Antenna for Space–Based Radars", CRC Report 1409, December 1986.

5. Tam W. and D. Faubert, "Displaced Phase Center Antenna Clutter Suppression in Space–Based Radar Applications", IEE Radar 1987 Digest.p. 385.

6. Faubert, D. and W. Tam, "Improvement in the Detection Performance of a Space–Based Radar Using a Displaced Phase Centre Antenna", 1987 International Symposium Digest Antenna and Propagation, June 1987, p. 914.

7. Lightstone, L., "A Model of a Displaced Phase Centre Antenna System for Space–Based Radar with Generalized Orbital Parameters and Earth Rotation." Atlantis Scientific Systems Group Inc., July 1987.

8. Tam, W. and D. Faubert. "High Order Displaced Phase Center Antenna for Space–Based Radar Applications". In preparation.

9. Ward, H. R., "Clutter Filter Performance Measures", IEEE International Conference, 1980, pp 231–239.

UNCLASSIFIED
_____
SECURITY CLASSIFICATION OF FORM
(highest classification of Title, Abstract, Keywords)

-25-

DOCUMENT CONTROL DATA

(Security classification of title, body of abstract and indexing annotation must be entered when the overall document is classified)

1. ORIGINATOR (the name and address of the organization preparing the document Organizations for whom the document was prepared, e.g. Establishment sponsoring a contractor's report, or tasking agency, are entered in section 8.) Radar Division DREO	2. SECURITY CLASSIFICATION (overall security classification of the document, including special warning terms if applicable) UNCLASSIFIED

3. TITLE (the complete document title as indicated on the title page. Its classification should be indicated by the appropriate abbreviation (S.C.R or U) in parentheses after the title.)

The Performance of Space-Based Radars Orbiting on Elliptical Orbits.

4. AUTHORS (Last name, first name, middle initial)

D. Faubert and M.P. Kerr

5. DATE OF PUBLICATION (month and year of publication of document) December 1988	6a. NO. OF PAGES (total containing information. Include Annexes, Appendices, etc.) 26	6b. NO. OF REFS (total cited in document) 9

7. DESCRIPTIVE NOTES (the category of the document, e.g. technical report, technical note or memorandum. If appropriate, enter the type of report, e.g. interim, progress, summary, annual or final. Give the inclusive dates when a specific reporting period is covered.)

Technical Report 88-995

8. SPONSORING ACTIVITY (the name of the department project office or laboratory sponsoring the research and development. Include the address.)

9a. PROJECT OR GRANT NO. (if appropriate, the applicable research and development project or grant number under which the document was written. Please specify whether project or grant) 021LA12	9b. CONTRACT NO. (if appropriate, the applicable number under which the document was written)

10a. ORIGINATOR'S DOCUMENT NUMBER (the official document number by which the document is identified by the originating activity. This number must be unique to this document.)	10b. OTHER DOCUMENT NOS. (Any other numbers which may be assigned this document either by the originator or by the sponsor)

11. DOCUMENT AVAILABILITY (any limitations on further dissemination of the document, other than those imposed by security classification)

(X) Unlimited distribution

( ) Distribution limited to defence departments and defence contractors; further distribution only as approved

( ) Distribution limited to defence departments and Canadian defence contractors; further distribution only as approved

( ) Distribution limited to government departments and agencies; further distribution only as approved

( ) Distribution limited to defence departments; further distribution only as approved

( ) Other (please specify):

12. DOCUMENT ANNOUNCEMENT (any limitation to the bibliographic announcement of this document. This will normally correspond to the Document Availability (11). However, where further distribution (beyond the audience specified in 11) is possible, a wider announcement audience may be selected.)

13. ABSTRACT (a brief and factual summary of the document. It may also appear elsewhere in the body of the document itself. It is highly
desirable that the abstract of classified documents be unclassified. Each paragraph of the abstract shall begin with an indication of the
security classification of the information in the paragraph (unless the document itself is unclassified) represented as (S), (C), (R), or (U).
It is not necessary to include here abstracts in both offical languages unless the text is bilingual).

The performance of Space-Based Radars (SBR) orbiting on elliptical orbits is
discussed. Their ability to detect air-breathing targets is analyzed as a
function of the antenna look angle, the orbital parameters of the satellite,
the number of radio pulses transmitted and the peak power of the radar.

The results show that the minimum detectable velocities of the SBR tend to
degrade as the satellite approaches the apogee of its orbit. Depending on the
orbital parameters of the satellite, the advantage of more extended coverage
when the satellite is at the apogee of its orbit could be hindered by the poorer
performance of the radar.

14. KEYWORDS, DESCRIPTORS or IDENTIFIERS (technically meaningful terms or short phrases that characterize a document and could be
helpful in cataloguing the document. They should be selected so that no security classification is required. Identifiers, such as equipment
model designation, trade name, military project code name, geographic location may also be included. If possible keywords should be selected
from a published thesaurus. e.g. Thesaurus of Engineering and Scientific Terms (TEST) and that thesaurus-identified. If it is not possible to
select indexing terms which are Unclassified, the classification of each should be indicated as with the title.)

Radar, Modelling, Space-Based, Simulation Elliptical Orbits.